Supporting Information

Bio-based porphyrins pyropheophorbide *a* and its Zn-complex as performing visible-light photosensitizers for free-radical photopolymerization

Louise Breloy,[a] Vlasta Brezová,[b] Sebastien Richeter,[c] Sébastien Clément,[c] Jean-Pierre Malval,[d] Samir Abbad-Andaloussi[e] and Davy-Louis Versace*[a]

[a] Institut de Chimie et des Matériaux Paris-Est (ICMPE) UMR CNRS 7182 UPEC, 2-8 rue Henri dunant, 94320 Thiais, France

[b] Slovak University of Technology in Bratislava, Institute of Physical Chemistry and Chemical Physics, Department of Physical Chemistry, Radlinského 9, SK-812 37 Bratislava, Slovak Republic.

[c] ICGM, Univ Montpellier, CNRS, ENSCM, Montpellier, France.

[d] Institut de Science des Matériaux de Mulhouse, UMR CNRS 7361, Université de Haute Alsace, 15 rue Jean Starcky, Mulhouse, 68057, France

[e] Université Paris-Est Créteil (UPEC), Laboratoire Eau, Environnement, Systèmes Urbains (LEESU), UMR-MA 102, 61 avenue Général de Gaulle, 94010 Créteil Cedex, France.

***Corresponding author**: versace@icmpe.cnrs.fr or davy-louis.versace@u-pec.fr

CONTENTS

FIGURES

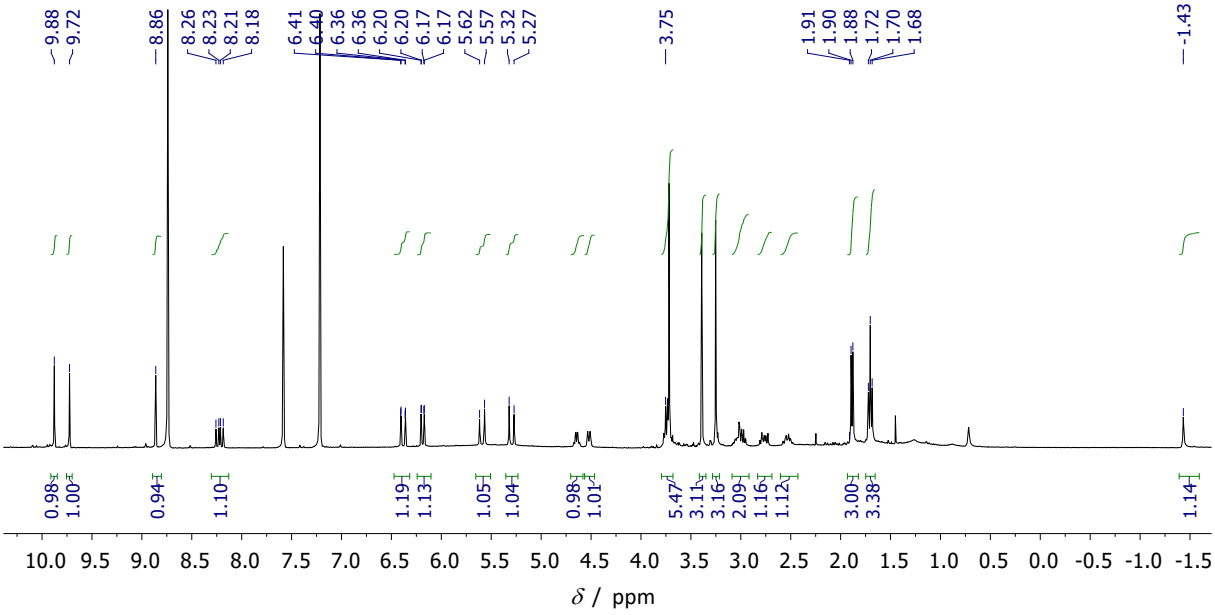

Figure S1. ^{1}H NMR spectrum (400 MHz, pyridine-d_5) of **Pyro**.

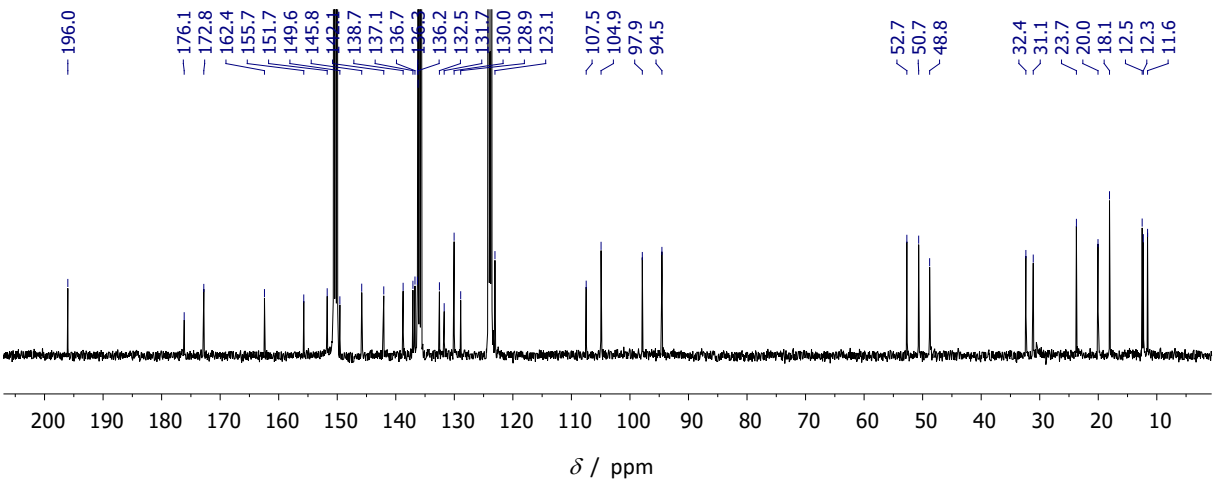

Figure S2. ^{13}C NMR spectrum (101 MHz, pyridine-d_5) of **Pyro**.

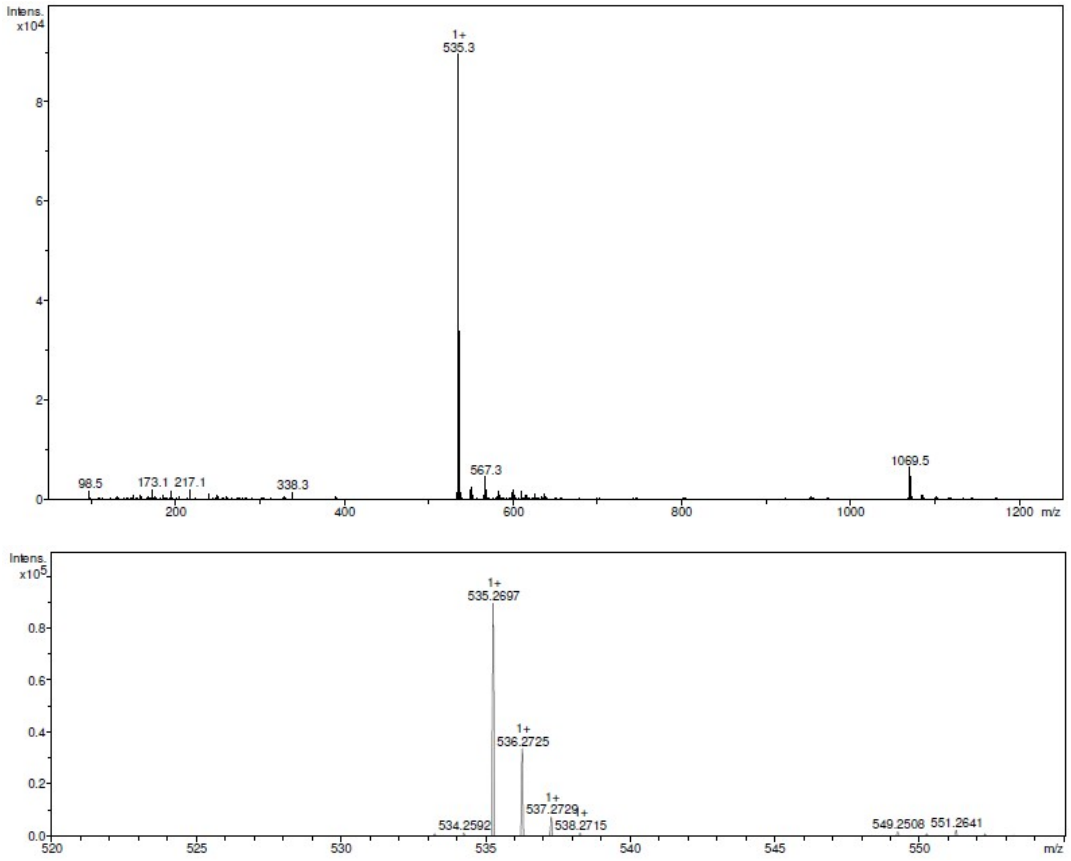

Figure S3. HR ESI-TOF mass spectrum (positive mode) of **Pyro**.

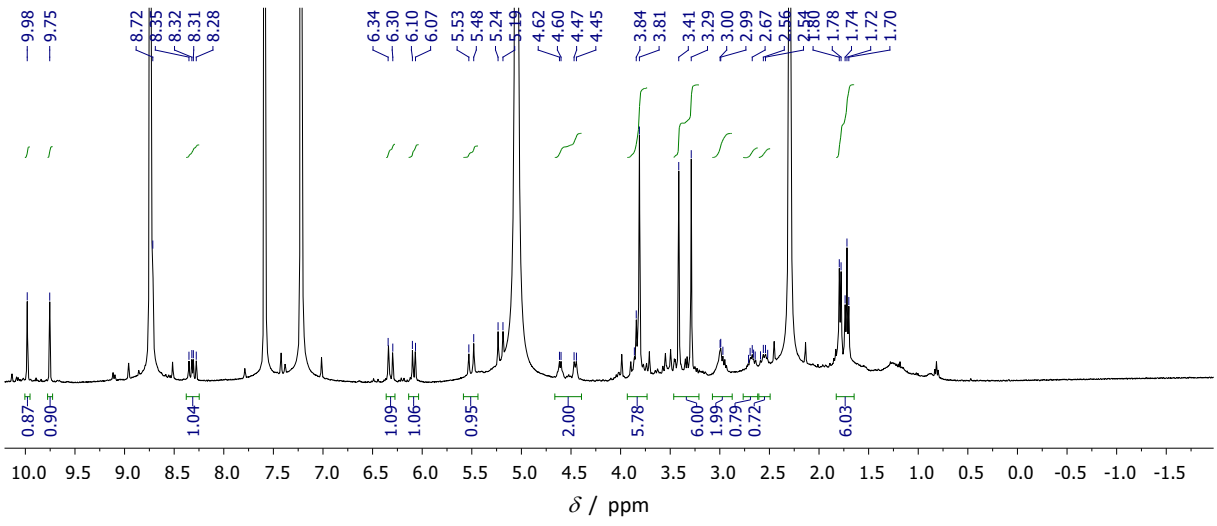

Figure S4. ^{1}H NMR spectrum (400 MHz, pyridine-d_5) of **Zn-Pyro**.

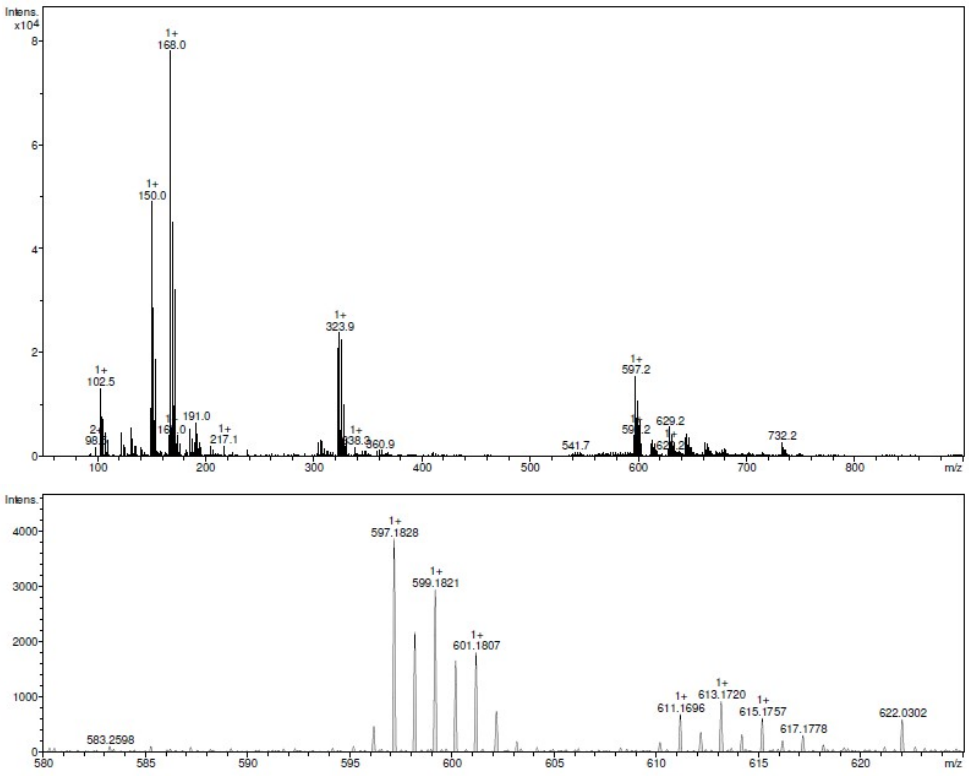

Figure S5. HR ESI-TOF mass spectrum (positive mode) of **Zn-Pyro**.

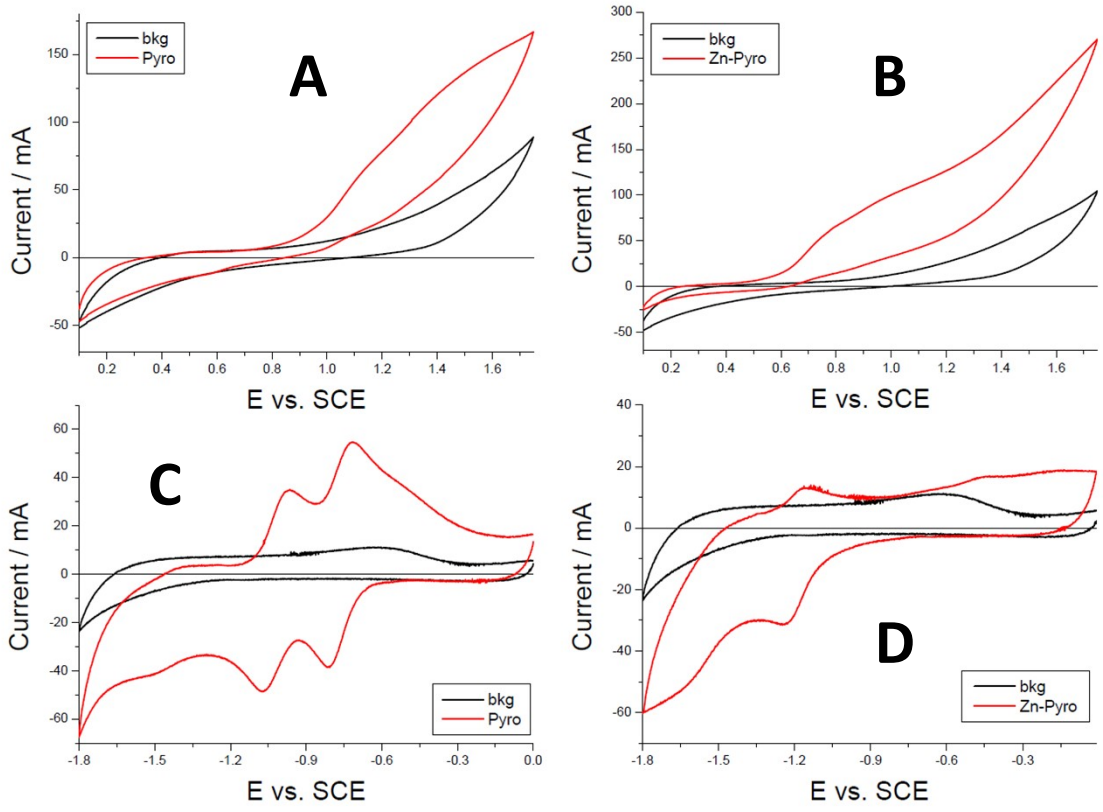

Figure S6. Cyclic voltammetry of **Pyro** (A, C) and **Zn-Pyro** (B, D) in DMF.

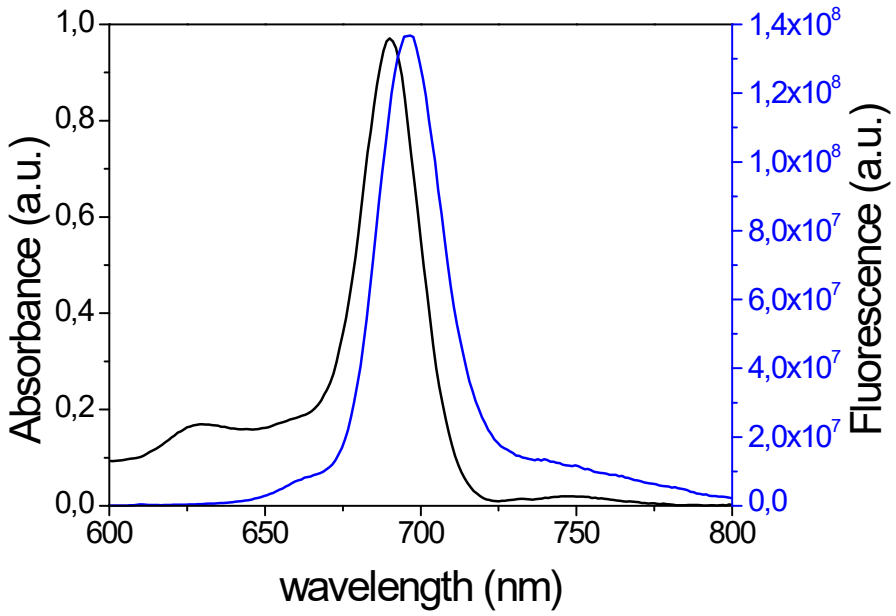

Figure S7. Absorption and fluorescence spectrum of **Pyro**.

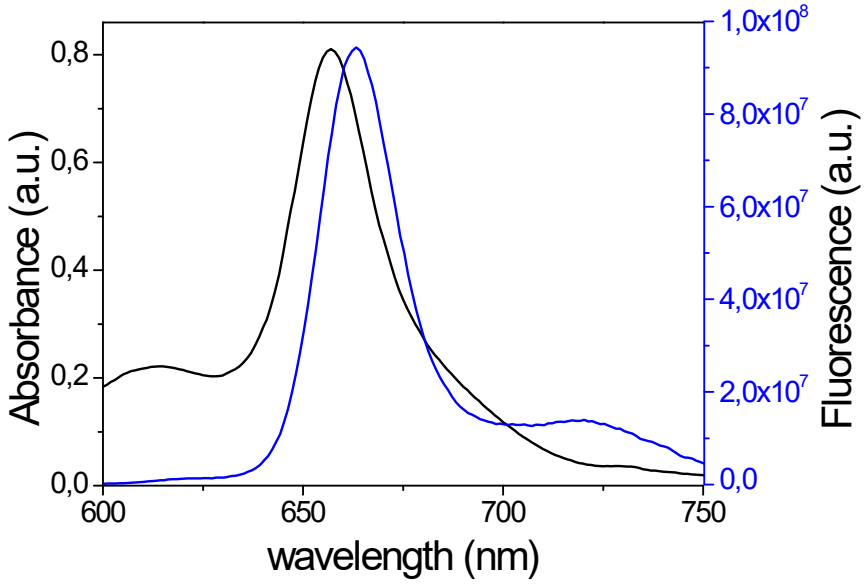

Figure S8. Absorption and fluorescence spectrum of **Zn-Pyro**.

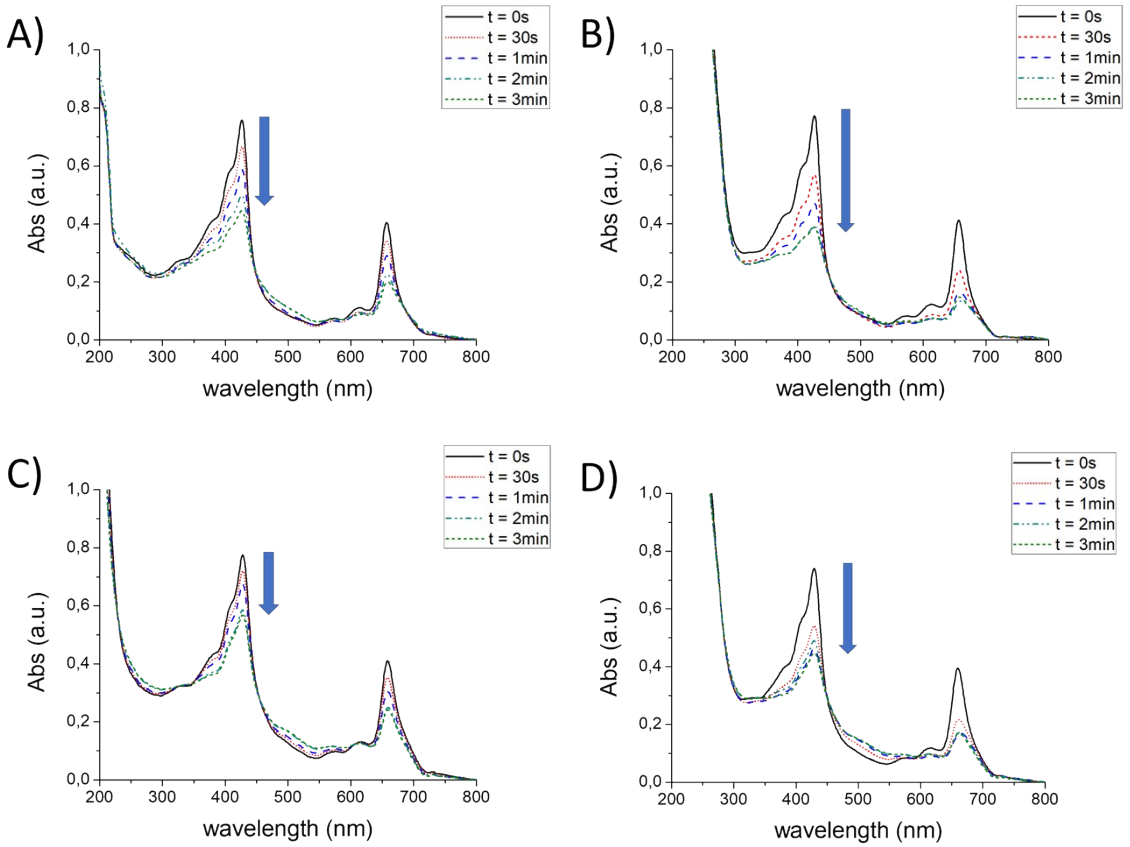

Figure S9. Photolysis of Zn-Pyropheophorbide a ([**Zn-Pyro**] = 1.5×10^{-5} M) (A) alone; (B) in the presence of Iod ([Iod]= 8×10^{-5} M); (C) in the presence of MDEA ([MDEA] = 1.1×10^{-4} M); and (D) in the presence of Iod and MDEA ([Iod] = 8×10^{-5} M and [MDEA] = 1.1×10^{-4} M) in ACN under LED@405 nm. Intensity = 25 mW.cm^{-2}.

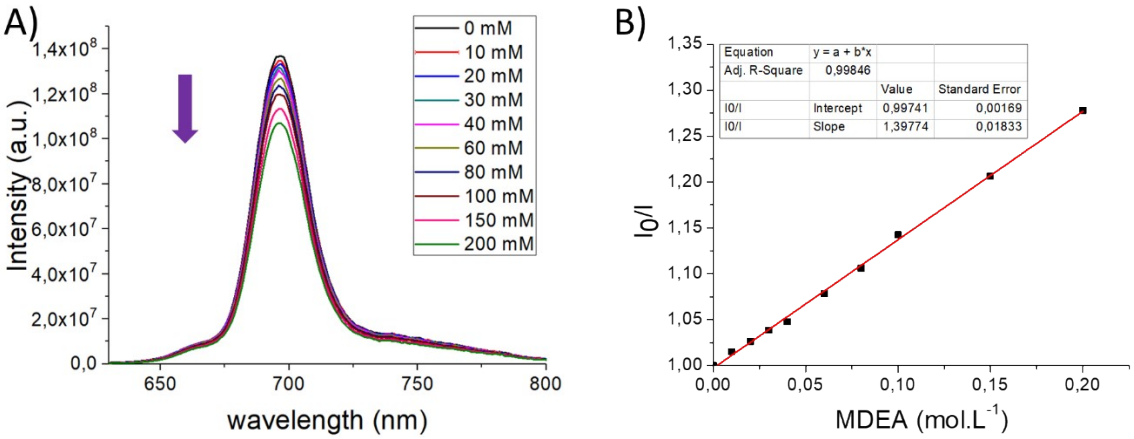

Figure S10. Quenching of fluorescence of **Pyro** upon gradual addition of MDEA in ACN (λ_{ex} = 420 nm): (A) fluorescence spectrum and (B) corresponding Stern-Volmer plot.

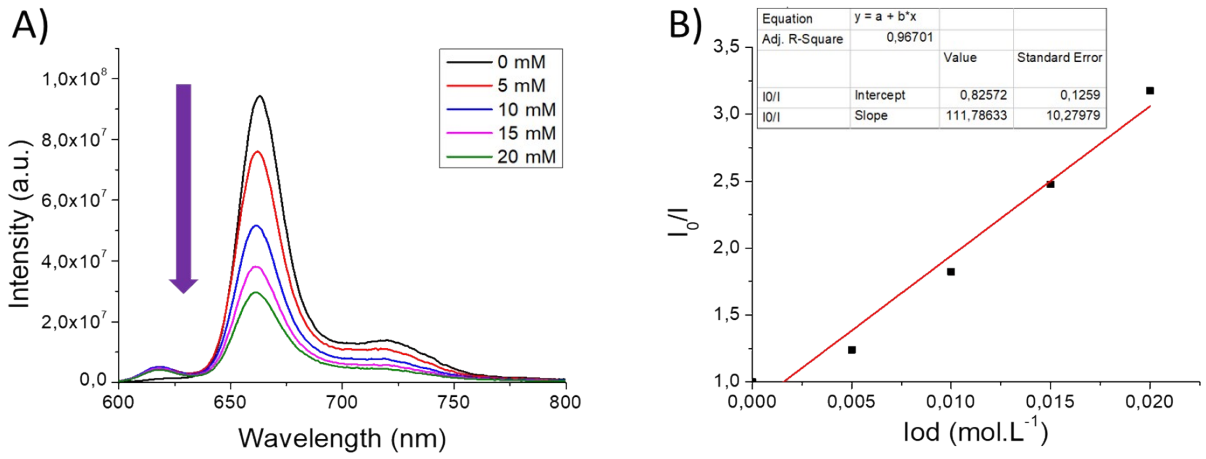

Figure S11. Quenching of fluorescence of **Zn-Pyro** upon gradual addition of Iod in ACN (λ_{ex}= 430 nm): (A) fluorescence spectrum and (B) corresponding Stern-Volmer plot.

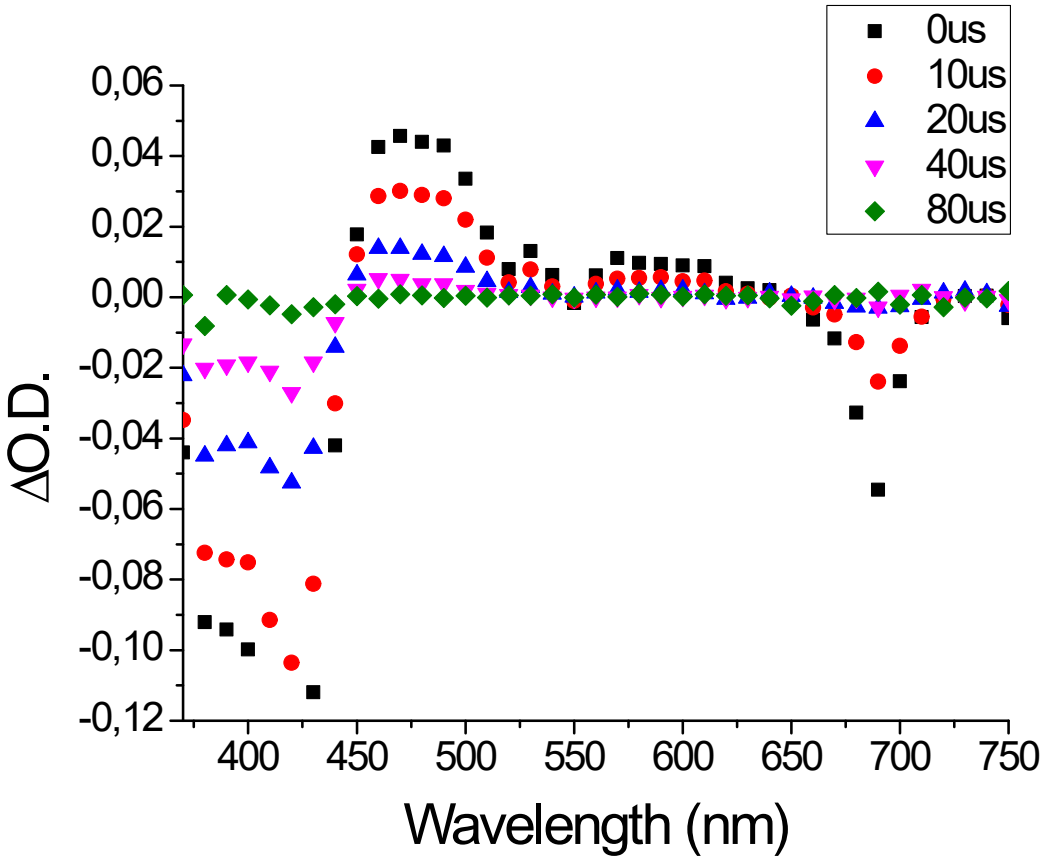

Figure S12. Transition absorption spectrum of the **Pyro** at t = 0, 10, 20, 40 and 80 μs under argon atmosphere (λ_{ex} = 355 nm) in ACN.

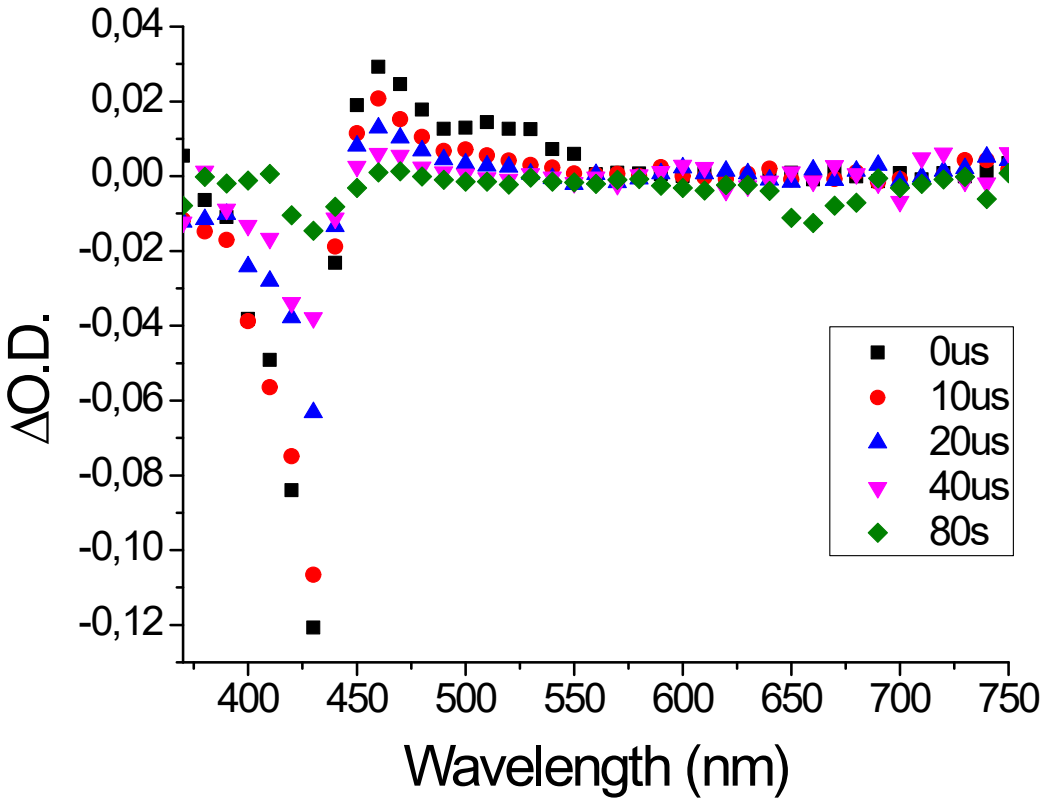

Figure S13. Transition absorption spectrum of **Zn-Pyro** at t = 0, 10, 20, 40 and 80 μs under argon atmosphere (λ_{ex} = 355 nm) in ACN.

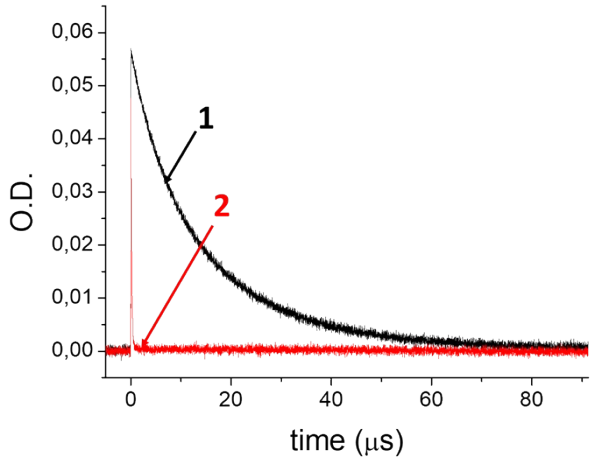

Figure S14. Transient absorption signal of **Pyro** at 470 nm (1) under argon atmosphere and (2) in oxygen-saturated conditions in ACN.

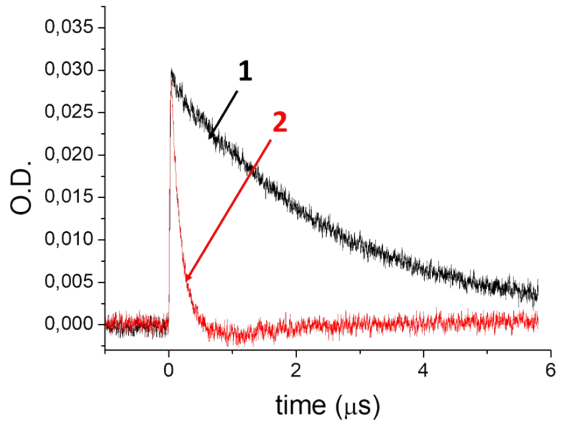

Figure S15. Transient absorption signal of **Zn-Pyro** at 460 nm (1) under argon atmosphere and (2) in oxygen-saturated conditions in ACN.

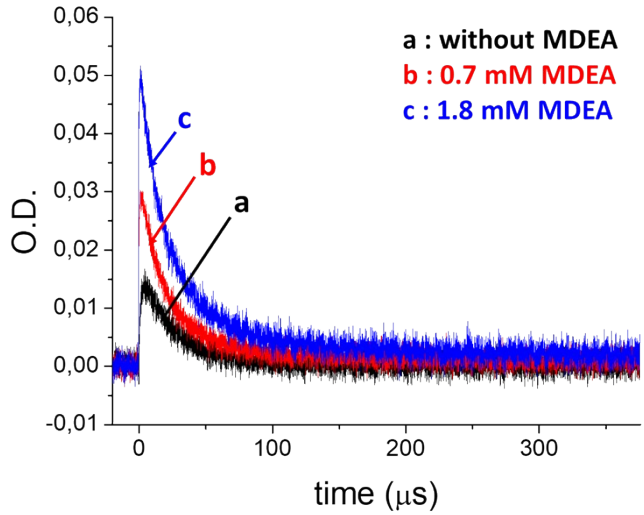

Figures S16. Transient absorption signal of **Zn-Pyro** in presence of different concentrations of MDEA at 460 nm in ACN.

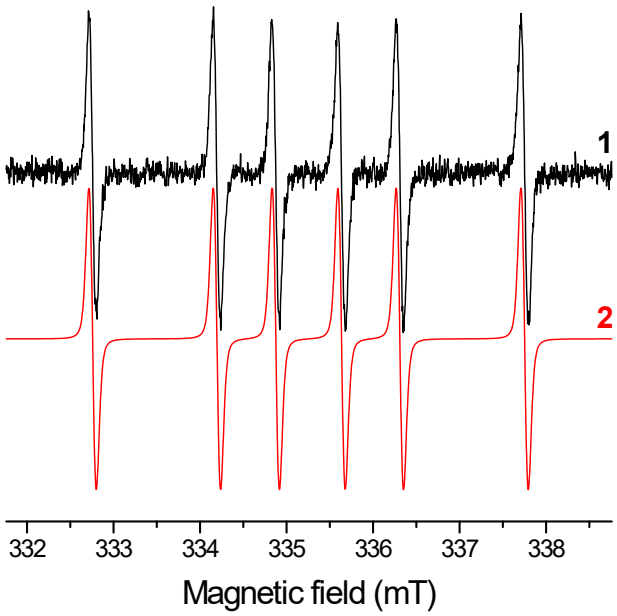

Figure S17. The normalized experimental (1) and simulated (2) EPR spectra obtained upon 450-s *in situ* LED@400 nm exposure of **Pyro**/Iod/ACN solutions in the presence of DMPO spin trap under argon. EPR spectrometer settings: microwave frequency, ~ 9.443 GHz; microwave power, 10.03 mW; center field, ~335.3 mT; sweep width, 7 mT; gain, 1.00×10^5; modulation amplitude, 0.025 mT; sweep time, 45 s; time constant, 10.24 ms; number of scans, 10.

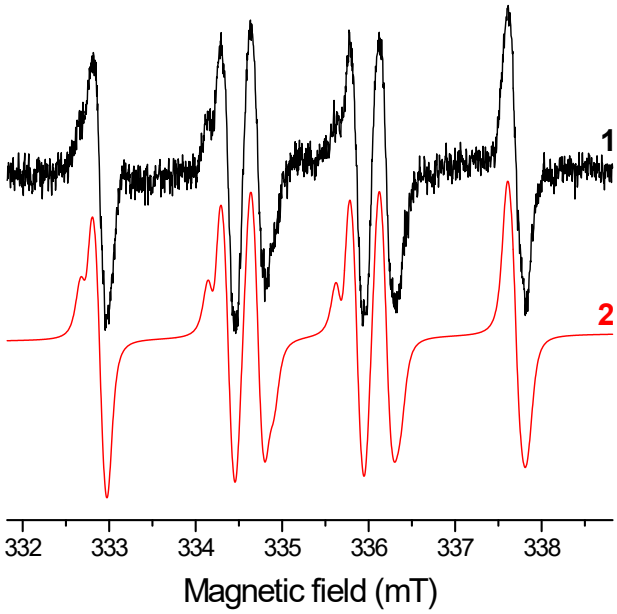

Figure S18. The normalized experimental (1) and simulated (2) EPR spectra obtained upon 1350-s *in situ* LED@400 nm exposure of **Pyro**/MDEA/ACN solutions in the presence of DMPO spin trap under argon. EPR spectrometer settings: microwave frequency, ~ 9.443 GHz;

microwave power, 10.01 mW; center field, ~335.3 mT; sweep width, 7 mT; gain, 1.00×10^5; modulation amplitude, 0.1 mT; sweep time, 45 s; time constant, 10.24 ms; number of scans, 10.

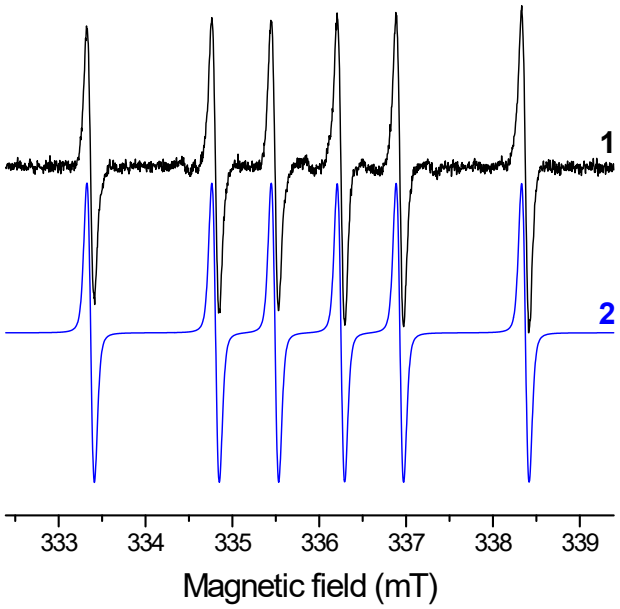

Figure S19. The normalized experimental (1) and simulated (2) EPR spectra obtained upon 450-s *in situ* LED@400 nm exposure of **ZnPyro**/Iod/ACN solutions in the presence of DMPO spin trap under argon. EPR spectrometer settings: microwave frequency, ~ 9.430 GHz; microwave power, 10.77 mW; center field, ~335.8 mT; sweep width, 7 mT; gain, 1.00×10^4; modulation amplitude, 0.025 mT; sweep time, 45 s; time constant, 10.24 ms; number of scans, 10.

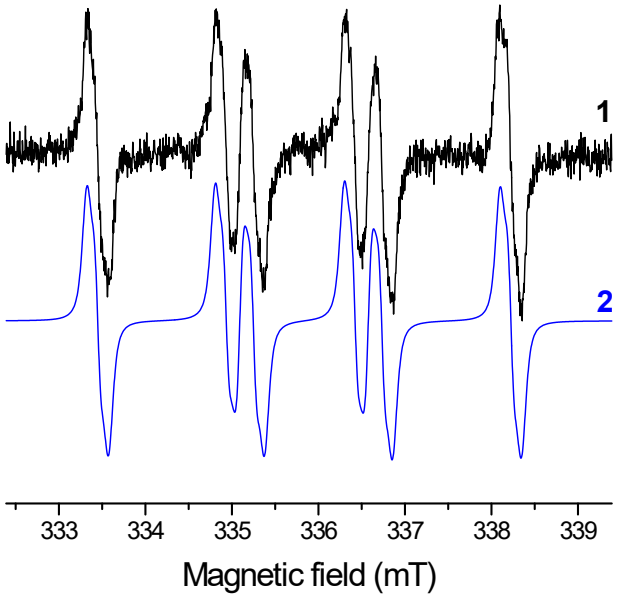

Figure S20. The normalized experimental (1) and simulated (2) EPR spectra obtained upon 1125-s *in situ* LED@400 nm exposure of **ZnPyro**/MDEA/ACN solutions in the presence of DMPO spin trap under argon. EPR spectrometer settings: microwave frequency, ~ 9.428 GHz; microwave power, 10.62 mW; center field, ~335.8 mT; sweep width, 7 mT; gain, 1.00×10^5; modulation amplitude, 0.05 mT; sweep time, 45 s; time constant, 10.24 ms; number of scans, 10.

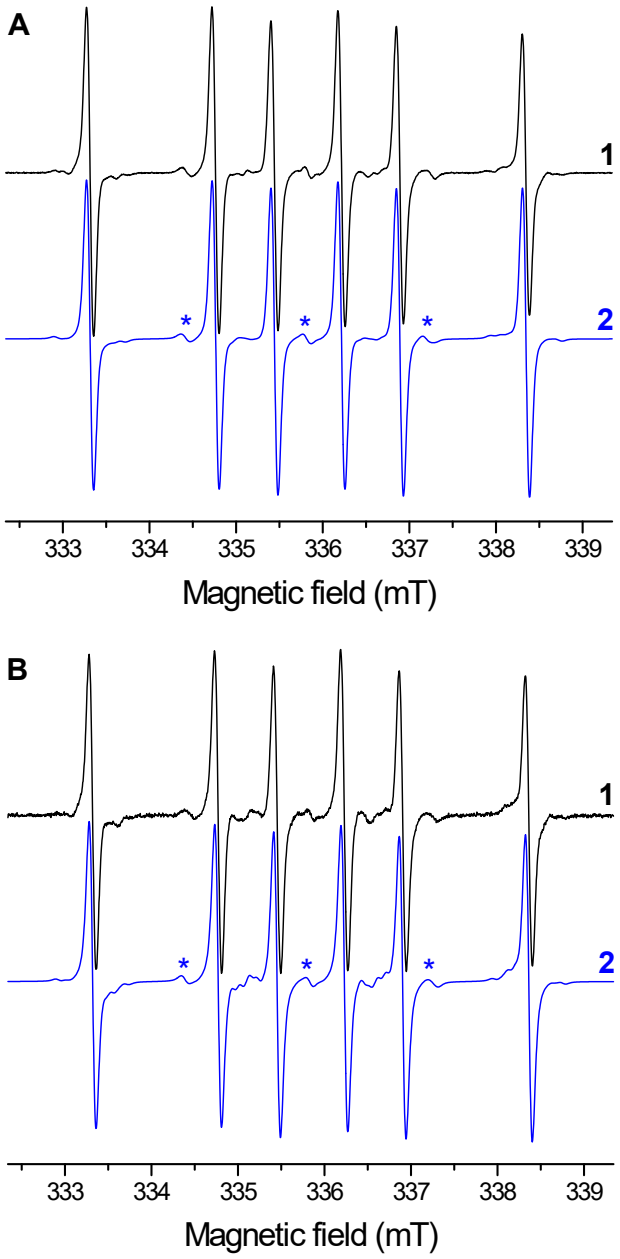

Figure S21. The normalized experimental (1) and simulated (2) EPR spectra obtained in **ZnPyro**/Iod/MDEA/ACN solutions in the presence of DMPO spin trap under argon upon *in situ* LED@400 nm exposure: (**A**) 225 s; (**B**) 1125 s. EPR spectrometer settings: microwave frequency, ~ 9.429 GHz; microwave power, 10.75 mW; center field, ~335.9 mT; sweep width, 7 mT; gain, 1.00×10^4; modulation amplitude, 0.025 mT; sweep time, 45 s; time constant, 10.24 ms; number of scans, 5. The three-line signal (*) represents DMPO degradation product.

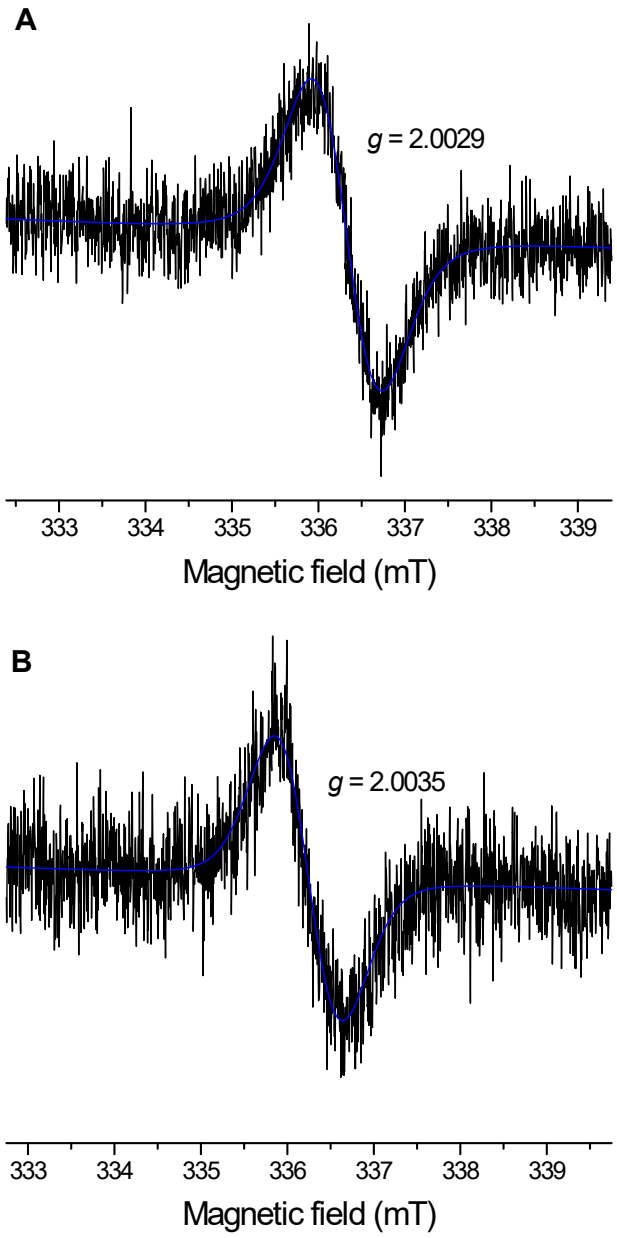

Figure S22. The normalized EPR spectra obtained upon 225 s *in situ* LED@400 nm exposure of photoinitiating systems in acetonitrile under argon: (**A**) **ZnPyro**/Iod; (**B**) **ZnPyro**/MDEA. EPR spectrometer settings: microwave frequency, ~ 9.428 GHz; microwave power, 10.72 mW; center field, ~336.2 mT; sweep width, 7 mT; gain, 1.00×10^5; modulation amplitude, 0.1 mT; sweep time, 45 s; time constant, 10.24 ms; number of scans, 5.

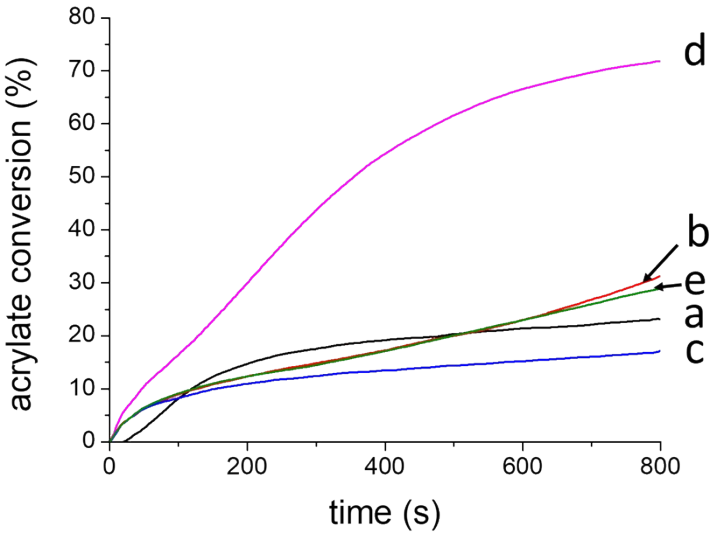

Figure S23. Kinetic profiles of PEGDA free-radical photopolymerization in the presence of PS/Cys (0.2%/0.8% w/w) with PS = **Pyro** (a) under air upon LED@405 nm, (b) under laminate upon LED@405 nm, (c) under laminate upon LED@455 nm or with PS = **Zn-Pyro** (d) under laminate upon LED@405 nm and (e) under laminate upon LED@455 nm.

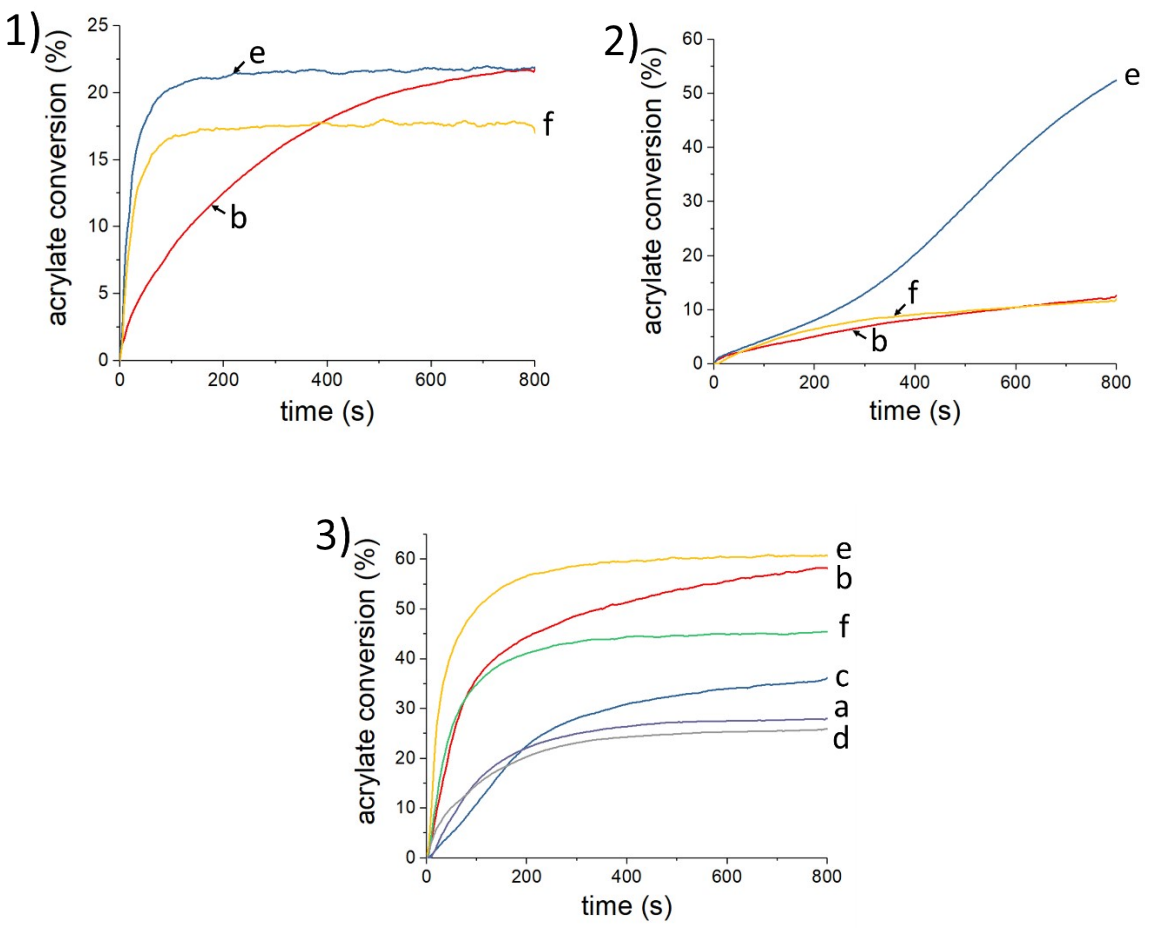

Figure S24. Kinetic profiles of PEGDA free-radical photopolymerization in the presence of (1) PS/MDEA (0.2%/0.8% w/w), (2) PS/Iod (0.2%/3% w/w) and (3) PS/Iod/MDEA (0.2%/3%/0.8% w/w/w) with PS = **Pyro** (a) under air upon LED@625 nm, (b) under laminate upon LED@625 nm, (c) under laminate upon LED@660 nm or with PS = **Zn-Pyro** (d) under air upon LED@625 nm, (e) under laminate upon LED@625 nm, and (f) under laminate upon LED@660 nm.

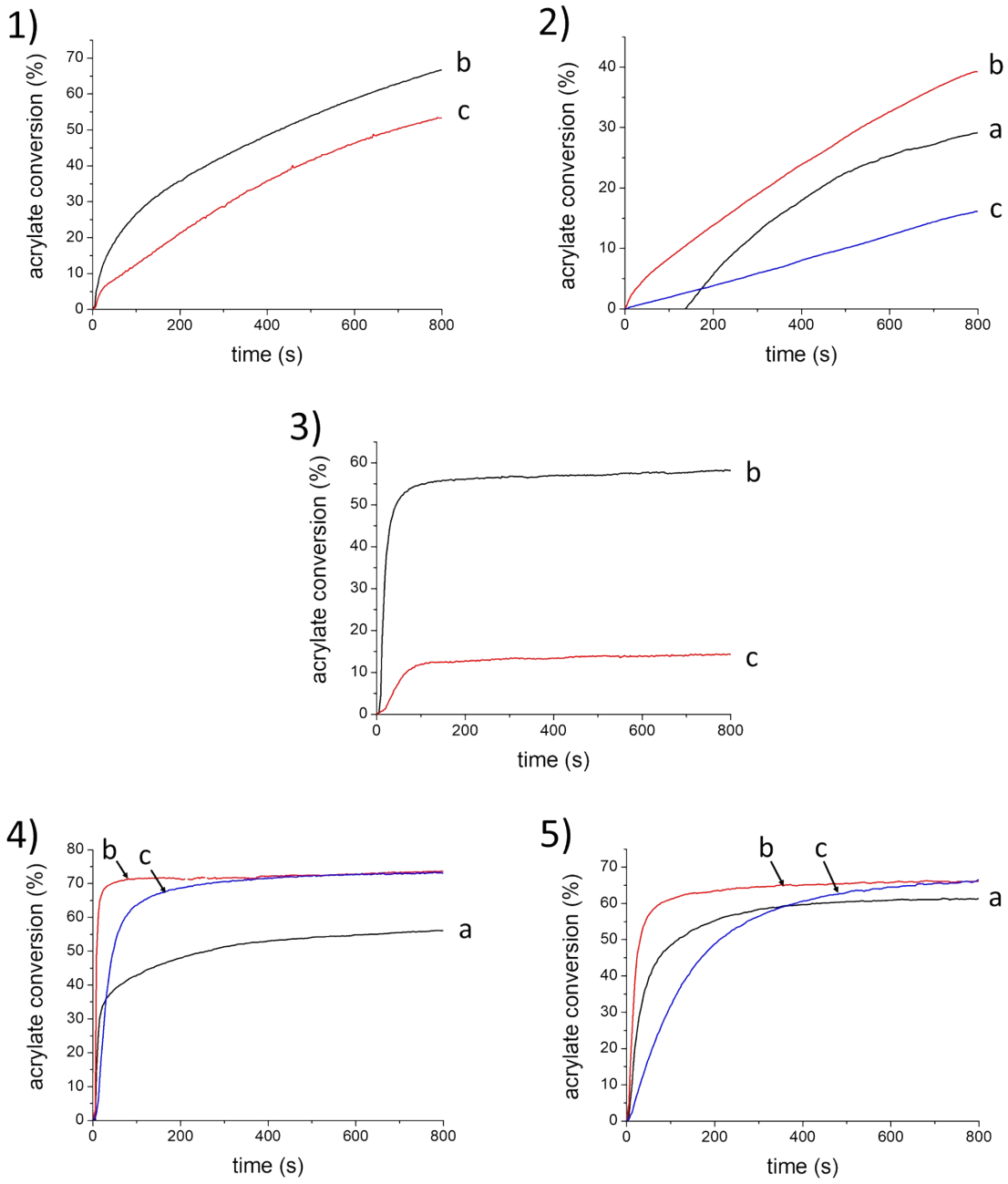

Figure S25. Kinetic study of PEGDA free-radical photopolymerization in the presence of (1) TPP/MDEA (0.2%/0.8% w/w), (2) TPP/Cys (0.2%/0.8% w/w), (3) TPP/Iod (0.2%/3% w/w), (4) TPP/Iod/MDEA (0.2%/3%/0.8% w/w/w) and (5) TPP/Iod/Cys (0.2%/3%/0.8% w/w/w) (a) under air upon LED@405 nm, (b) under laminate upon LED@405 nm, (c) under laminate upon LED@455 nm.

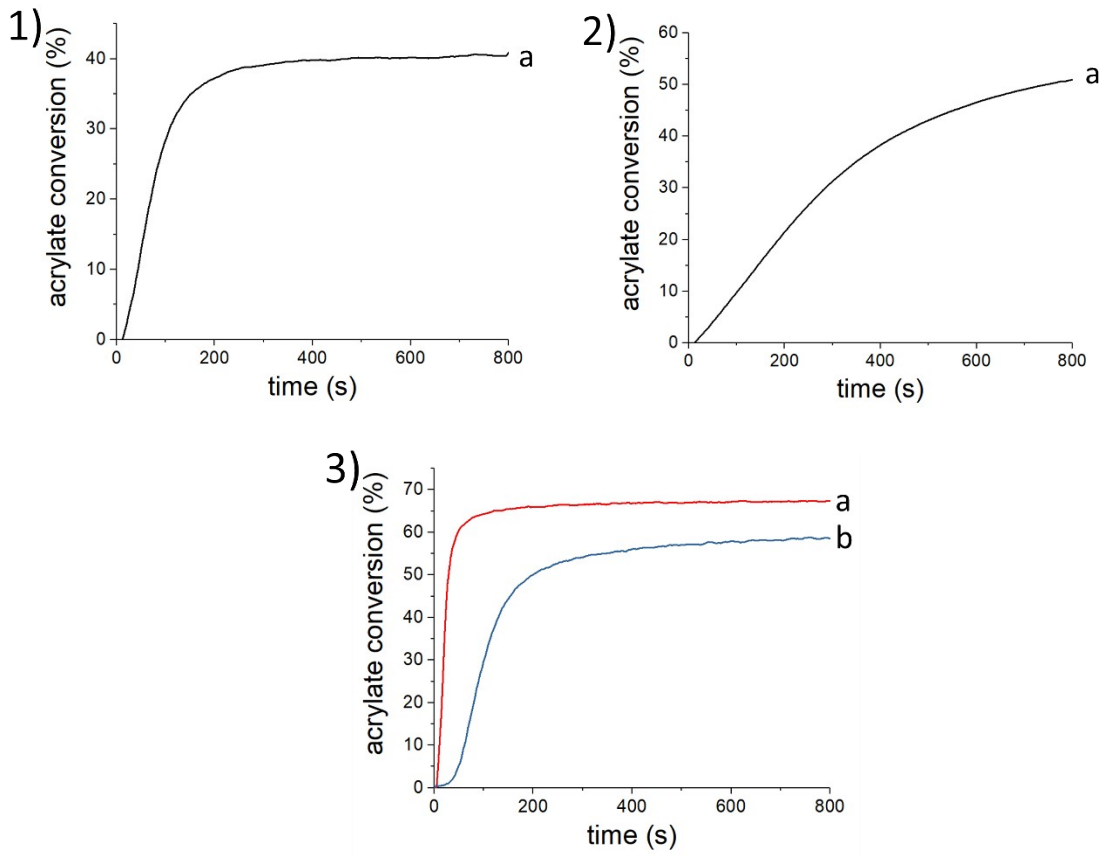

Figure S26. Kinetic study of PEGDA free-radical photopolymerization in the presence of (1) TPP/MDEA (0.2%/0.8% w/w), (2) TPP/Iod (0.2%/3% w/w), and (3) TPP/Iod/MDEA (0.2%/3%/0.8% w/w/w) (a) under laminate upon LED@625 nm, (c) under laminate upon LED@660 nm.

TABLES

Table S1. The spin-Hamiltonian parameters of DMPO spin-adducts elucidated from the simulations of the experimental EPR spectra measured upon LED@400 nm irradiation of **Pyro** and **ZnPyro** in the deoxygenated acetonitrile solutions

DMPO-adduct	a_N **(mT)**	a_H **(mT)**	***g*-factor**
•DMPO-phenyl(4-methyl)[a]	1.454±0.009	2.134±0.009 (H^{β})	2.0059±0.0001
•DMPO-CR(aminoalkyl)	1.494±0.006	1.804±0.014 (H^{β}) 0.103±0.010 (H^{γ}) 0.078(±0.010H^{γ})	2.0059±0.0001

[a] ^{13}C satellites in mT: 0.807±0.012, 0.757±0.015, 0.618±0.015, 0.557±0.012[1]

Table S2. Initial rates of PEGDA polymerization $(R_P/[M]_0)\,x10^2$ in the presence of systems (1) PS/amine (0.2%/0.8% w/w), (2) PS/Iod (0.2%/3% w/w) and (3) PS/Iod/amine (0.2%/3%/0.8% w/w/w) with PS = **Pyro** or **Zn-Pyro**

Photoinitiating systems	**405 nm**	**455 nm**	**625 nm**	**660 nm**
(1) PS/amine				
TPP/MDEA	np[a], 0.89[b]	np[a], 0.31[b]	np[a], 0.12[b]	np[a], np[b]
TPP/Cys	0.09[a], 0.14[b]	np[a], 0.02[b]	-	-
Pyro/MDEA	0.05[a], 0.94[b]	np[a], 0.01[b]	np[a], 0.03[b]	np[a], np[b]
Pyro/Cys	0.11[a], 0.18[b]	np[a], 0.18[b]	-	-
Zn-Pyro/MDEA	np[a], 0.05[b]	np[a], np[b]	np[a], 0.04[b]	np[a], 0.03[b]
Zn-Pyro/Cys	np[a], 0.27[b]	np[a], 0.18[b]	-	-
(2) PS/Iod				
TPP/Iod	np[a], 2.45[b]	np[a], 0.24[b]	np[a], 0.32[b]	np[a], np[b]
Pyro/Iod	np[a], 0.08[b]	np[a], 0.08[b]	np[a], 0.18[b]	np[a], np[b]
Zn-Pyro/Iod	np[a], 4.00[b]	np[a], 1.23[b]	np[a], 0.72[b]	np[a], 0.52[b]
(3) PS/Iod/amine				
TPP/Iod/MDEA	3.67[a], 16.20[b]	np[a], 1.00[b]	np[a], 1.78[b]	np[a], 0.04[b]

TPP/Iod/Cys	1.28[a], 2.9[b]	np[a], 0.34[b]	-	-
Pyro/Iod/MDEA	np[a], 3.77[b]	np[a], 0.96[b]	0.22[a], 0.46[b]	np[a], 0.10[b]
Pyro/Iod/DMA	0.15[a], 0.62[b]	np[a], 0.09[b]	-	-
Pyro/Iod/BDMA	np[a], 2.98[b]	np[a], 2.75[b]	-	-
Pyro/Iod/Ribo	np[a], 0.25[b]	np[a], 0.07[b]	-	-
Pyro/Iod/Cys	0.18[a], 0.18[b]	np[a], 0.54[b]	-	-
Pyro/Iod/Argi	0.33[a], 0.98[b]	np[a], 0.21[b]	-	-
Zn-Pyro/IodMDEA	0.37[a], 10.93[b]	1.79[a], 9.73[b]	0.30[a], 1.13[b]	np[a], 0.60[b]
Zn-Pyro/Iod/DMA	0.27[a], 2.36[b]	np[a], 6.27[b]	-	-
Zn-Pyro/Iod/BDMA	np[a], 4.53[b]	np[a], 9.63[b]	-	-
Zn-Pyro/Iod/Ribo	np[a], 1.00[b]	np[a], 0.20[b]	-	-
Zn-Pyro/Iod/Cys	2.60[a], 6.05[b]	0.16[a], 2.61[b]	-	-
Zn-Pyro/Iod/Argi	np[a], 2.51[b]	np[a], 1.67[b]	-	-

Table S3. Oxidation potentials of amine co-initiators (V).

	E_{ox} (V)
MDEA	1.0[2]
DMA	0.8[3]
BDMA	0.74[4]
Ribo	1.5[5]
Cys	0.92[6]
Argi	0.65[7]

SCHEMES

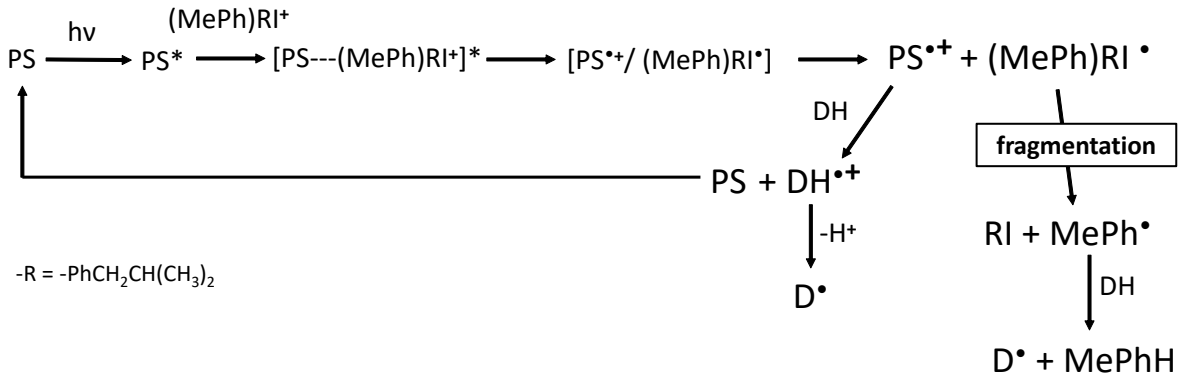

Scheme S1. Photooxidizable mechanism of initiation by a three-component photoinitiating system.

EQUATIONS

Equation S1. Rehm-Weller equation.

$$\Delta G_{et} = F \times (E_{ox}(\text{Donor}) - E_{red}(\text{Acceptor})) - E_S \text{ (or } E_T) + \Delta E_c \quad \text{(S1)}$$

with E_{ox} (Donor), E_{red} (Acceptor), E_S (or E_T), ΔEc and F are respectively the oxidation potential of the donor (MDEA, **Pyro** or **ZnPyro**), the reduction potential of the acceptor (Iod, Pyro or ZnPyro), the excited singlet (or triplet) state energy of the sensitizer (**Pyro** or **Zn-Pyro**), the Coulombic stabilization energy (negligible for most systems) and Faraday constant.

REFERENCES

1. D. Barasch, J. Katzhendler, M. C. Krishna, A. Russo and A. Samuni, *J. Am. Chem. Soc.* , 1994, **116**, 7319.
2. D. Kim and J. W. Stansbury, *J. Polym. Sci. Part A: Polym. Chem.*, 2009, **47**, 3131.
3. T. L. Macdonald, W. G. Gutheim, R. B. Martin and F. P. Guengerich, *Biochem. 1989,* **28**, 2071.
4. M. Masui, H. Sayo and Y. Tsuda, *J. Chem. Soc. B: Phys. Org.*, 1968, DOI: 10.1039/j29680000973, 973.
5. K. A. Korvinson, G. N. Hargenrader, J. Stevanovic, Y. Xie, J. Joseph, V. Maslak, C. M. Hadad and K. D. Glusac, *J. Phys. Chem. A*, 2016, **120**, 7294.
6. I. El-Hallag, A. O. Al-Youbi, A. Y. Obaid, E. H. El-Mossalamy, S. A. El-Daly and A. M. Asiri, *J. Chil. Chem. Soc.*, 2011, **56**, 837.
7. H. Heli, N. Sattarahmady and M. Hajjizadeh, *Anal. Methods*, 2014, **6**, 6981.